



**HAL**  
open science

## Extraction of tori from minimal point sets

Laurent Busé, André Galligo

► **To cite this version:**

| Laurent Busé, André Galligo. Extraction of tori from minimal point sets. 2017. hal-01553065v1

**HAL Id: hal-01553065**

**<https://inria.hal.science/hal-01553065v1>**

Preprint submitted on 3 Jul 2017 (v1), last revised 8 Dec 2017 (v2)

**HAL** is a multi-disciplinary open access archive for the deposit and dissemination of scientific research documents, whether they are published or not. The documents may come from teaching and research institutions in France or abroad, or from public or private research centers.

L'archive ouverte pluridisciplinaire **HAL**, est destinée au dépôt et à la diffusion de documents scientifiques de niveau recherche, publiés ou non, émanant des établissements d'enseignement et de recherche français ou étrangers, des laboratoires publics ou privés.

# Extraction of tori from minimal point sets

Laurent Busé<sup>1</sup> and André Galligo<sup>2</sup>

<sup>1</sup>Université Côte d’Azur, Inria, France.

<sup>2</sup>Université Côte d’Azur, Laboratoire J.-A. Dieudonné and Inria, France.

July 3, 2017

## Abstract

A new algebraic method for extracting tori from a minimal point set, made of two oriented points and a simple point, is proposed. We prove a degree bound on the number of such tori; this bound is reached on examples, even when we restrict to smooth tori. Our method is based on pre-computed closed formulae well suited for numerical computations with approximate input data.

**Keywords:** mixed set of 3D points, tori, interpolation method.

## 1 Introduction

The extraction of geometric primitives from 3D point clouds is an important problem in reverse engineering. These 3D point clouds are typically obtained by means of accurate 3D scanners and there exists several methods for performing the 3D geometric primitives extraction. An important category among them are based on a RANSAC method [3, 7, 8]. The basic idea is to extract a particular elementary type of shape, such as planes, spheres, cylinders, cones or tori, from the smallest possible set of points and then to judge if this extracted primitive is relevant to the full point cloud. Therefore, it is very important to compute a particular type of shape through the smallest possible number of points, including normals if available. While extraction of planes and spheres is easy to treat, the cases of cylinders and cones are more difficult. In a previous work [1] we proposed a detailed analysis and efficient algorithms for these basic surfaces. In this note we treat the case of tori which is much more involved. More precisely, we provide a new method for extracting tori from the smallest possible number of points, counting multiplicities of oriented points. Here, such a minimal point set is made of two oriented points and a simple point, which account for seven parameters, i.e. the same number as the degrees of freedom of the considered problem.

In the sequel, an *oriented point* is a couple of a point and a nonzero vector. A surface is said to interpolate an oriented point if the point belongs to the surface and its associated vector is colinear to the normal of the surface at this point. Notice that we are not assuming that the orientation of the normal of the point is the same as the orientation of the surface. Moreover, it is important to deal with inhomogeneous data, that is to say some points are oriented but not all, in order to take into account the estimated accuracy of oriented point clouds that are obtained by means of normal estimation algorithms. A set of data made of points and oriented points is called a mixed set of points.

Previous approaches to the extraction of elementary geometric primitives have been treated from an overdetermined number of points (counting multiplicities) and hence produce estimated shapes that are not exactly interpolating the data; see e.g. [6]. For instance, in [4, 5] tori are extracted, more precisely estimated, from three points with normals (three points with normals impose nine conditions, and in general there is no torus that interpolate such data). In [1], we proposed efficient extraction algorithms for the case of cylinders

and cones from a minimum number of independent conditions, which is seven, is achieved. At the heart of this contribution is an original and subtle modelisation of this interpolation problem (opposed to brute force computations). Based on this modelisation, our approach relies on adapted algebraic techniques and allows to develop an efficient extraction algorithm in the context of numerical computations in double precision with approximate data. In section 3, we will prove the following theorem.

**Theorem.** *There exist at most eight non-degenerated tori (or an infinity) that interpolate three distinct points, two of them being oriented.*

Our strategy of proof relies on geometric constructions related to 3D interpolation of circles which are described in Section 2. In Section 4, we will report on our numerical experiments, and also show an example for which this upper bound (eight) is reached, even when we restrict to smooth tori, which is the useful practical setting.

## 2 3D circles passing through two oriented points

The spine of a torus is a 3D circle. Such a circle depends on six parameters : three parameters for the coordinates of its center, two parameters for its supporting plane and one last parameter corresponding to its radius. Thus 3D circles and pairs of oriented points share the same number of degrees of freedom, namely six, and hence one may ask how many circles pass through two oriented points.

**Proposition 1.** *We suppose that two distinct points  $A_1$  and  $A_2$  and two nonzero vectors  $N_1$  and  $N_2$  are given. For  $i = 1, 2$ , we denote by  $\Omega_i$  the intersection point, possibly at infinity, between the bisecting plane of the segment  $[A_1 A_2]$  and the line passing through  $A_i$  and parallel to  $N_i$  (see Figure 1). Consider the following fitting problem (P): determine all the 3D circles that interpolate  $A_1$  and  $A_2$  and which are normal to  $N_1$  at  $A_1$  and normal to  $N_2$  at  $A_2$ .*

- (a) *If  $\Omega_1 \neq \Omega_2$  and  $\Omega_1, \Omega_2$  are not both at infinity, then there is one and only one circle that satisfies (P).*
- (b) *If  $\Omega_1 \neq \Omega_2$  and  $\Omega_1, \Omega_2$  are both at infinity, then there is no circle that satisfies (P).*
- (c) *If  $\Omega_1 = \Omega_2$  then there are infinitely many circles that satisfy (P).*

*Proof.* First, we observe that a 3D circle  $\mathcal{C}$  defines a sheaf of spheres whose centers belong to the line  $L$  passing by the center of  $\mathcal{C}$  and orthogonal to its supporting plane. Suppose that a point  $A$  on  $\mathcal{C}$  and a nonzero vector  $N$  are given. Denote by  $D$  the line through  $A$  and parallel to  $N$ . Then,  $N$  is orthogonal to  $\mathcal{C}$  at  $A$  if and only if  $N$  is orthogonal at  $A$  to one and only one of the spheres of the sheaf associated to  $\mathcal{C}$ , namely the one whose center is the intersection point between the lines  $D$  and  $L$ . We notice that if  $D$  and  $L$  are parallel lines, i.e. if  $N$  is normal to the supporting plane of  $\mathcal{C}$ , then the corresponding "limit sphere" of the sheaf of spheres has to be seen as the supporting plane of  $\mathcal{C}$ , since its center is at infinity and its radius is infinite.

Now, returning to our fitting problem, let  $\mathcal{C}$  be a circle that interpolates the two distinct points  $A_1$  and  $A_2$ . By the previous observation, we have that the vector  $N_1$  is normal to  $\mathcal{C}$  at  $A_1$  if and only if  $N_1$  is normal at  $A_1$  to the sphere  $S_1$  whose center is  $\Omega_1$  and that goes through  $A_1$ . In other words, the vector  $N_1$  is normal to  $\mathcal{C}$  at  $A_1$  if and only if  $\mathcal{C}$  is contained in the sphere  $S_1$ . Similarly, the vector  $N_2$  is normal to  $\mathcal{C}$  at  $A_2$  if and only if  $\mathcal{C}$  is contained in the sphere  $S_2$  whose center is  $\Omega_2$  and that goes through  $A_2$ . We recall that if  $\Omega_1$ , respectively  $\Omega_2$ , is at infinity then  $S_1$ , respectively  $S_2$ , is the normal plane to  $N_1$  through  $A_1$ , respectively the normal plane to  $N_2$  through  $A_2$ .

To conclude the proof we see that if  $\Omega_1 \neq \Omega_2$  and  $\Omega_1, \Omega_2$  are not both at infinity then the intersection of  $S_1$  and  $S_2$  defines a unique circle because this is the intersection of two spheres, or a sphere and a plane, which contains the two distinct points  $A_1$  and  $A_2$ . If  $\Omega_1 \neq \Omega_2$  and  $\Omega_1, \Omega_2$  are both at infinity then  $S_1$  and  $S_2$  are two distinct planes whose intersection is the line through  $A_1$  and  $A_2$ , so there is no solution to (P) in this case. Finally, if  $\Omega_1 = \Omega_2$  then  $S_1$  and  $S_2$  are both the same sphere, or the same plane, and hence any circle on this sphere, or on this plane, that goes through  $A_1$  and  $A_2$  will give a solution to (P).  $\square$

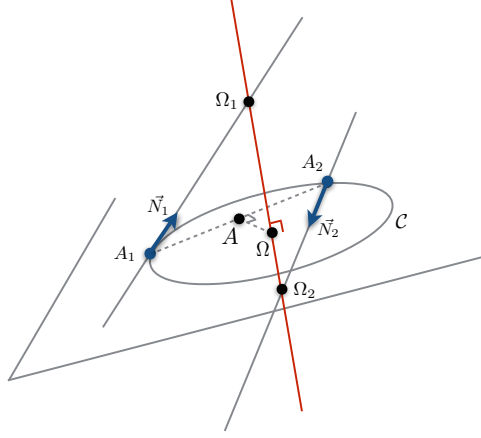


Figure 1: Fitting a 3D circle passing through two distinct points with normal directions.

The above geometric constructions can be quantified to provide explicit formulae that we will use in the next section. Without loss of generality, one may assume that  $N_1$  and  $N_2$  are unitary vectors, which we will do in this section.

**Case  $(a_1)$ .** We begin with a sub-case of the first item of Proposition 1, that we denote  $(a_1)$ :  $\Omega_1 \neq \Omega_2$  and neither  $\Omega_1$  nor  $\Omega_2$  is at infinity. Let  $\Omega_1 := A_1 + \lambda_1 N_1$  and  $\Omega_2 := A_2 + \lambda_2 N_2$ . We have  $\|\overrightarrow{\Omega_1 A_1}\|^2 = \|\Omega_1 A_2\|^2$  and  $\|\overrightarrow{\Omega_2 A_1}\|^2 = \|\Omega_2 A_2\|^2$ . Let  $A$  denotes the middle of  $A_1$  and  $A_2$  (see Figure 1). Since  $\overrightarrow{\Omega_1 A} \cdot \overrightarrow{A_1 A_2} = 0$  and  $\overrightarrow{\Omega_1 \Omega} \cdot \overrightarrow{A_1 A_2} = 0$ , we deduce that  $\overrightarrow{\Omega_1 A_1} + \frac{1}{2} \overrightarrow{A_1 A_2} \cdot \overrightarrow{A_1 A_2} = 0$  and we get

$$\lambda_1 = \frac{\|\overrightarrow{A_1 A_2}\|^2}{2\overrightarrow{N_1} \cdot \overrightarrow{A_1 A_2}}, \quad \lambda_2 = \frac{\|\overrightarrow{A_1 A_2}\|^2}{2\overrightarrow{N_2} \cdot \overrightarrow{A_2 A_1}}. \quad (1)$$

Now, the center  $\Omega$  of the circle  $\mathcal{C}$  satisfies  $\|\overrightarrow{\Omega \Omega_1}\|^2 = \|\Omega_1 A_1\|^2 - \|A_1 \Omega\|^2 = \lambda_1^2 - R^2$ , and similarly for  $\Omega_2$ , where  $R$  stands for the radius of  $\mathcal{C}$ . Substituting in the expression of the squared norm of  $\overrightarrow{\Omega \Omega_2} = \overrightarrow{\Omega \Omega_1} + \overrightarrow{\Omega_1 \Omega_2}$ , we obtain  $\lambda_2^2 - R^2 = \lambda_1^2 - R^2 + \|\Omega_1 \Omega_2\|^2 + 2\overrightarrow{\Omega \Omega_1} \cdot \overrightarrow{\Omega_1 \Omega_2}$  and we deduce

$$\Omega = \Omega_1 + \frac{1}{2} \left( \frac{(\lambda_1^2 - \lambda_2^2)}{\|\overrightarrow{\Omega_1 \Omega_2}\|^2} + 1 \right) \overrightarrow{\Omega_1 \Omega_2}, \quad R^2 = \lambda_1^2 - \frac{1}{4} \frac{(\lambda_1^2 - \lambda_2^2 + \|\Omega_1 \Omega_2\|^2)^2}{\|\overrightarrow{\Omega_1 \Omega_2}\|^2}.$$

Symmetrizing these formulae we get

$$\Omega = \frac{\Omega_1 + \Omega_2}{2} + \frac{(\lambda_1^2 - \lambda_2^2)}{2} \frac{\overrightarrow{\Omega_1 \Omega_2}}{\|\overrightarrow{\Omega_1 \Omega_2}\|^2}, \quad 4R^2 = 4(\lambda_1^2 + \lambda_2^2) - \|\Omega_1 \Omega_2\|^2 - \frac{(\lambda_1^2 - \lambda_2^2)^2}{\|\overrightarrow{\Omega_1 \Omega_2}\|^2}. \quad (2)$$

Expressing the previous formulae with coordinates reveals unexpected algebraic properties which will be useful in the next section. Choosing an adapted frame, we can let  $A_1$  be the origin,  $N_1 = (0, 0, 1)$ ,  $N_2 = (l, m, n)$ , and  $A_2 = (0, y_2, z_2)$ . It follows that

$$\|\overrightarrow{A_1 A_2}\|^2 = y_2^2 + z_2^2, \quad \overrightarrow{N_1} \cdot \overrightarrow{A_1 A_2} = z_2, \quad \overrightarrow{N_2} \cdot \overrightarrow{A_2 A_1} = my_2 + nz_2.$$

Then, simple formal computations which could be done by hand but are easier with a computer algebra system yields the following properties.

**Lemma 2.** *Using the above notation, the quantity*

$$S = 4 \frac{\|\overrightarrow{\Omega_1 \Omega_2}\|^2}{\|\overrightarrow{A_1 A_2}\|^2} \cdot (\overrightarrow{N_1} \cdot \overrightarrow{A_1 A_2}) \cdot (\overrightarrow{N_2} \cdot \overrightarrow{A_2 A_1})$$

is a polynomial in the input parameters, namely

$$S = l^2(y_2^2 z_2^2 + z_2^4) + m^2(y_2^2 - z_2^2)^2 + 4mny_2 z_2(y_2^2 - z_2^2) + 4n^2 y_2^2 z_2^2.$$

In addition, the following properties hold:

i)  $4 \cdot S \cdot R^2 = \|A_1 A_2\|^2 (S + l^2 y_2^2 (y_2^2 + z_2^2)).$

iii) the coordinates of  $S \cdot \overrightarrow{\Omega M}$  are polynomials in the input parameters,

ii) the quantity  $(\overrightarrow{\Omega_1 \Omega_2} \cdot \overrightarrow{\Omega M}) \cdot (\overrightarrow{N_1} \cdot \overrightarrow{A_1 A_2}) \cdot (\overrightarrow{N_2} \cdot \overrightarrow{A_2 A_1})$  is a polynomial in the input parameters, namely

$$X (ly_2^2 z_2 + lz_2^3) + Y(-my_2^2 z_2 + mz_2^3 - 2ny_2 z_2^2) + Z(my_2^3 - my_2 z_2^2 + 2ny_2^2 z_2).$$

This latter quantity provides a reduced equation of the supporting plane of the circle  $C$ .

**Case (a<sub>2</sub>).** Now, consider the case where  $\Omega_1$  is at infinity but not  $\Omega_2$ . Then the unique circle solution of the fitting problem is the intersection of the plane normal to  $N_1$  and the sphere at  $\Omega_2$ , both passing through  $A_1$ . With the previously chosen notation for the frame and the coordinates, we now have  $z_2 = 0$ ,  $y_2 \neq 0$  and  $m \neq 0$ . A straightforward computation shows that the equation of the plane containing the circle is  $Z = 0$  and in this plane the equation of the circle (multiplied by  $4m^2$  which is nonzero) is

$$(2mX - ly_2)^2 + (2mY - y_2 m)^2 = m^2 y_2^2 + l^2 y_2^2.$$

Thus, its center  $\Omega$  and the square of its radius  $R$  are given by

$$\Omega = \left( \frac{-ly_2}{2m}, \frac{y_2}{2}, 0 \right), \quad R^2 = \frac{y_2^2(l^2 + m^2)}{4m^2}.$$

We also notice that the quantity  $S$  defined in Lemma 2, case (a<sub>1</sub>), specializes when  $z_2 = 0$  to  $S = m^2 y_2^4$  which is nonzero. Actually, the specialization of the entire Lemma 2 is still valid so that it can always be applied when the 3D circle fitting problem admits a unique solution.

Therefore, case (a<sub>2</sub>) does not require a specific treatment compared to the case (a<sub>1</sub>) when dealing with explicit formulae.

**Cases (b) and (c).** In case (b) there is no solution and this case can be detected with the following test :  $z_2 = 0$ ,  $y_2 \neq 0$ , and  $m = 0$ ,  $l \neq 0$ . In case (c) there are infinitely many solutions and it can be detected with the following test :  $m^2 = 2ln$  and  $m \neq 0$ ; or  $z_2 = 0$  and  $l = m = 0$ .

We notice that the stronger condition “ $m \neq 0$  and  $m^2 \neq 2ln$ ” excludes both cases (b) and (c) and only depends on the input normals ( $N_1$  and  $N_2$ ).

### 3 Tori passing through a minimal point set

A torus is defined as the set of points in the three-dimensional affine space  $\mathbb{R}^3$  that are located at a fixed distance, called the *small radius* of the torus, of a given circle which is called the *skeletal circle* of the torus; the radius of this circle will be called the *big radius* of the torus and will be denoted by  $R$ , while the small radius will be denoted by  $r$ . Seven parameters are needed for a torus: six for its skeletal circle and an additional one for the small radius.

Below, we will prove our main theorem; i.e. we will solve the problem of computing the tori passing through three distinct points, two of them being oriented. These points form a minimal point set because they correspond to seven conditions. Thus, our input consists in three distinct points  $P_1, P_2, P_3$  and two nonzero normal vectors  $N_1, N_2$  that are attached to the points  $P_1, P_2$ .

**Implicit equations of tori.** The points of a torus are exactly those points that are at distance  $r$ , the small radius of the torus, to the skeletal circle of the torus, which is a 3D circle of center  $\Omega$  and radius  $R$ . We denote by  $\vec{N}$  a unitary normal vector to the supporting plane of the skeletal circle. The squared distance of a point  $M$  to the skeletal circle can be classically derived as

$$(\vec{N} \cdot \overrightarrow{\Omega M})^2 + \left( \sqrt{\|\Omega M\|^2 - (\vec{N} \cdot \overrightarrow{\Omega M})^2} - R \right)^2.$$

Since this latter quantity must be equal to  $r^2$  we obtain the following implicit equation of the torus:

$$4R^2 \left( \|\Omega M\|^2 - (\vec{N} \cdot \overrightarrow{\Omega M})^2 \right) = (\|\Omega M\|^2 + R^2 - r^2)^2.$$

In the sequel, we will need to drop the hypothesis that  $\vec{N}$  is a unitary vector. In this setting, the implicit equation of the torus becomes

$$\|N\|^2 (\|\Omega M\|^2 + R^2 - r^2)^2 - 4R^2 \left( \|N\|^2 \cdot \|\Omega M\|^2 - (\vec{N} \cdot \overrightarrow{\Omega M})^2 \right) = 0. \quad (3)$$

**Proof of the theorem.** First, by a change of coordinates we can assume that  $P_1$  is at the origin with  $N_1 = (0, 0, 1)$ , and also that  $P_2 = (0, y_2, z_2)$ . We set  $N_2 = (l, m, n)$  and  $P_3 = (x_3, y_3, z_3)$ .

We introduce two new quantities  $r_1$  and  $r_2$  and we consider the two points  $A_1 = P_1 + r_1 N_1$  and  $A_2 = P_2 + r_2 N_2$ . These two points will belong to the skeletal circle of a torus, of small radius equal to  $|r_1|$ , that interpolates the two oriented points  $P_1$  and  $P_2$  providing

$$r_1^2 = r_2^2 \|N_2\|^2 = r_2^2 (l^2 + m^2 + n^2). \quad (4)$$

Assume that we are in the first case of Proposition 1, i.e. the subcases  $(a_1)$  or  $(a_2)$ , and so that there is a unique circle that interpolates the points  $A_1$  and  $A_2$  and which is normal to  $N_1$  at  $A_1$  and normal to  $N_2$  at  $A_2$ . This circle is the skeletal circle of the interpolating torus. Taking again the notation of Section 2, we denote by  $\Omega = (a, b, c)$  its center, by  $R$  its radius and by  $\vec{N} := (u, v, w)$  which is a normal vector to the supporting plane of this circle. From Equation (3), (1) and (2), the implicit equation of this interpolating torus can be written in terms of the space coordinates  $x, y, z$  and on the parameters  $y_2, z_2, l, m, n$  and  $r_1, r_2$ . It turns out that, thanks to the algebraic remarks summarized in Lemma 2 of the previous section, this equation can be factorized and replaced by a simplified polynomial that we will denote by  $E$ . To be more precise, assume that we are in the case  $(a_1)$  and define the following polynomial quantities:

$$P := \|A_1 A_2\|^2 = r_2^2 l^2 + m^2 r_2^2 + n^2 r_2^2 + 2mr_2 y_2 - 2nr_1 r_2 + 2nr_2 z_2 + r_1^2 - 2r_1 z_2 + y_2^2 + z_2^2,$$

$$Q_1 := \overrightarrow{N_1} \cdot \overrightarrow{A_1 A_2} = nr_2 - r_1 + z_2, \quad Q_2 := \overrightarrow{N_2} \cdot \overrightarrow{A_2 A_1} = l^2 r_2 + m^2 r_2 + n^2 r_2 + m y_2 - n r_1 + n z_2.$$

Then, using the properties given in Lemma 2, straightforward symbolic computations show that the implicit equation of the torus (3) writes as

$$\frac{P}{Q_1^2 \cdot Q_2^2} \cdot E(x, y, z, x_2, y_2, l, m, n, r_1, r_2) \quad (5)$$

where  $E$  is a polynomial. Similar computations shows that this polynomial also encapsulates the case  $(a_2)$ . The polynomial equation  $E = 0$  is obviously of degree 4 in the variables  $x, y, z$ . It turns out that it is of degree 8 with respect to each of the variables  $l, m$ , of degree 6 with respect to each of the variables  $n, y_2, z_2, r_2$  and of degree 7 with respect to the variable  $r_1$ .

Summarizing the above calculations, the tori that interpolate the three distinct points  $P_1, P_2, P_3$ , where  $P_1$  are  $P_2$  are oriented by  $N_1$  and  $N_2$  respectively, are given by the two algebraic equations

$$E(x_3, y_3, z_3, x_2, y_2, l, m, n, r_1, r_2) = 0$$

(the variables  $x, y, z$  have been substituted by the point  $P_3$  in order to impose the interpolation condition at this point) and  $U := r_1^2 - r_2^2(l^2 + m^2 + n^2) = 0$  deduced from the condition (4). Since the polynomial  $U$  is monic in  $r_1$ , we can perform an Euclidian division of  $E$  by  $U$  with respect to variables  $r_1$ , which remainder is a polynomial in  $r_1$  of degree at most 1, that we denote by  $S_1 + r_1S_2$ . Then, the system of equations finally reduces to

$$S_1 + r_1S_2 = 0, \quad r_1^2 - r_2^2(l^2 + m^2 + n^2) = 0 \quad (6)$$

where  $S_1$  and  $S_2$  are polynomials in  $x_3, y_3, z_3, l, m, n, y_2, z_2, r_2$  of degree 4 and 3 respectively.

From here, the explicit expression shows that the elimination of  $r_1$  from these two equations yields a polynomial in  $x_3, y_3, z_3, l, m, n, y_2, z_2, r_2$  which is of degree 8 with respect to the variable  $r_2$ . Since the quantity  $x_3, y_3, z_3, l, m, n, y_2, z_2$  are input data, one can solve  $r_2$  from this equation and then build a unique torus for each of these values. Thus, we have proved the claimed theorem.

As illustrated in Figure 2, the upper bound of eight tori is reached on examples, even under the restriction of smooth tori. The input data corresponding to this illustration is  $P_1 = (0, 0, 0)$ ,  $N_1 = (0, 0, 1)$ ,  $P_2 = (0, -3.171791777, -2.369900007)$ ,  $N_2 = (-3.736353882, -2.170588024, 0.215631583)$  and  $P_3 = (-0.394882587, 3.246764454, -3.362188875)$ .

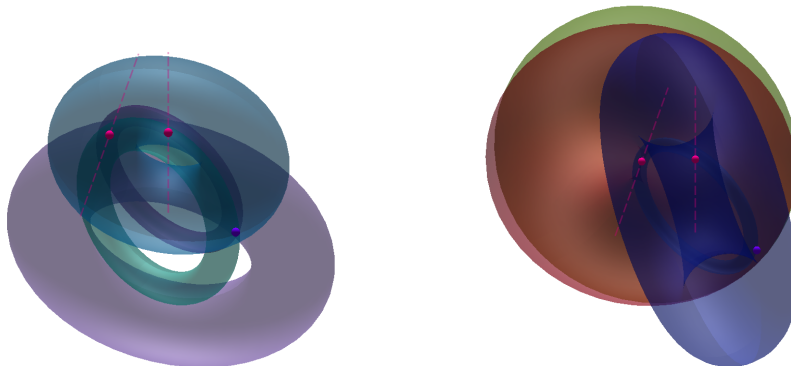


Figure 2: Eight tori that interpolate a minimal point set, separated into two groups of four torus in order to improve the visualization.

## 4 Effective solving and experiments

In order to apply the previous method for the extraction of tori in 3D point clouds by means of RANSAC-based approaches, we need to devise an algorithm that is fast and adapted to approximate data and numerical computations with double precision since this is the standard of the current libraries dealing with surface reconstruction.

The algebraic strategy we developed aims at producing closed form formulae that can be stored and used efficiently to solve the interpolation problem. Thus, the degree 8 polynomial in the variable  $r_2$  we found could be pre-computed and its coefficients could be stored. Then, for each particular instance this polynomial could be solved and the tori extracted. However, this is not what we did. Indeed, the coefficients of this polynomial are big polynomials and their evaluation in double precision with approximate data yield significant numerical instability. In order to overcome this difficulty, we use a matrix-based formulation of the elimination of the variable  $r_1$  in the system (6). More precisely, we form the Sylvester matrix of these two polynomials with respect to the variable  $r_1$ . This is a  $3 \times 3$ -matrix whose entries are polynomials of degree at most 4 in the variable  $r_2$ . Then, we compute its associated pencil of companion matrices  $A, B$  which are  $12 \times 12$  matrices. For each particular instance, the generalized eigenvalues and eigenvectors of these matrices

are computed to provide the couple of roots  $r_1, r_2$  of this system (see [1] or [2] for more details). In practice, the matrices  $A$  and  $B$  are pre-computed and stored. It turns out that their entries are of smaller size and degree compared to the coefficients of the above degree 8 polynomial in  $r_2$ . This and the use of generalized eigenvalues yield a much more numerically stable algorithm.

A prototype of the extraction algorithm we have described above has been implemented with the **Maple** software. We observed that the extraction of the tori from a random set of three points, two of them being oriented, takes in average 24ms and is almost constant independently of the point set. Some illustrative configurations are shown in Figure 3 and the proportion of the number of smooth tori (i.e. whose big radius is bigger than its small radius) found through such set of points is reported in Table 1. We emphasize that the case of eight distinct smooth tori that interpolate three given points, two being oriented, is effectively reached; see Figure 2 and Figure 4.

Number of smooth tori	0	1	2	3	4	5	6	7	8
Proportion (%)	7.98	39.42	29.71	16.61	5.01	0.77	0.47	0.02	0.01

Table 1: Proportion of the number of smooth tori found through ten thousands random point sets.

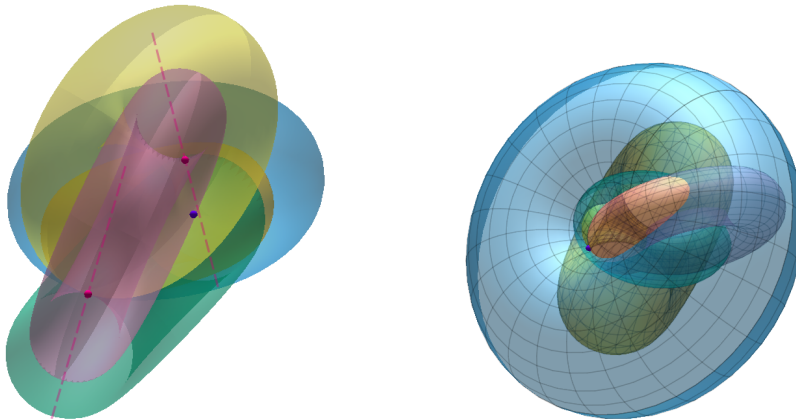


Figure 3: Two configurations of points with 4 interpolating smooth tori.

For the sake of completeness, we mention the following alternative strategy for solving the polynomial system (6). Since  $l, m, n$  are input data, the quantity  $r_1$  can be expressed in terms of  $r_2$  in two possible ways. For each of these two possible values, the other equation of the system then yields a univariate polynomial of degree 4 in  $r_2$  that can be solved by means of Ferrari’s method.

Another important point we would like to mention is on the practical use of our method. Unless the usual approaches (e.g. [3, 4, 7]), our method may output several tori for a given point set. An option to reduce this number of tori, typically to select only one or zero torus, is to use some additional information such as the normal at the third point  $P_3$  which is not used in our method. Indeed, it might be the case that this normal is expected to be in a certain cone and hence we can filter the tori we computed by comparing the normal vector at  $P_3$  for each torus with this cone.

## 5 Conclusion

This work continues our study of optimized basic shapes extraction from point clouds. We presented a point of view which combines geometric and algebraic aspects. The minimal (mixed) point set for defining a finite number of tori consists in two oriented points and a simple one, corresponding to seven numbers of freedom.



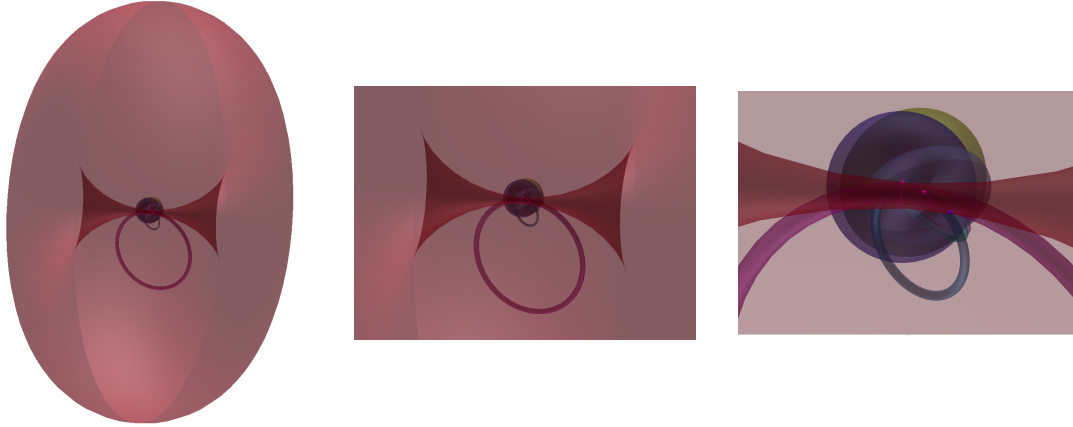


Figure 4: Eight smooth tori that interpolate a point set. The focus is increased from left to right in order to visualize all the eight tori.

We proposed an original analysis and an efficient algorithm for performing this extraction. Its main step consists of applying rather simple matrix-based closed formulae.

## References

- [1] Laurent Busé, André Galligo, and Jiajun Zhang. Extraction of cylinders and cones from minimal point sets. *Graphical Models*, 86:1–12, 2016.
- [2] Laurent Busé, Houssam Khalil, and Bernard Mourrain. Resultant-based methods for plane curves intersection problems. In Victor G. Ganzha, Ernst W. Mayr, and Evgenii V. Vorozhtsov, editors, *Computer Algebra in Scientific Computing (CASC)*, volume 3718, pages 75–92, Kalamata, Greece, September 2005. Springer Berlin / Heidelberg.
- [3] Martin A. Fischler and Robert C. Bolles. Random sample consensus: A paradigm for model fitting with applications to image analysis and automated cartography. *Commun. ACM*, 24(6):381–395, June 1981.
- [4] John R. Kender and Rick Kjeldsen. On seeing spaghetti: A novel self-adjusting seven parameter hough space for analyzing flexible extruded objects. In *Proceedings of the 12th International Joint Conference on Artificial Intelligence - Volume 2, IJCAI'91*, pages 1271–1277, San Francisco, CA, USA, 1991. Morgan Kaufmann Publishers Inc.
- [5] John R. Kender and Rick Kjeldsen. On seeing spaghetti: Self-adjusting piecewise toroidal recognition of flexible extruded objects. *IEEE Trans. Pattern Anal. Mach. Intell.*, 17(2):136–157, 1995.
- [6] Gabor Lukács, Ralph Martin, and Dave Marshall. Faithful least-squares fitting of spheres, cylinders, cones and tori for reliable segmentation. In Hans Burkhardt and Bernd Neumann, editors, *Computer Vision — ECCV'98*, volume 1406 of *Lecture Notes in Computer Science*, pages 671–686. Springer Berlin Heidelberg, 1998.
- [7] Ruwen Schnabel, Roland Wahl, and Reinhard Klein. Efficient ransac for point-cloud shape detection. *Computer Graphics Forum*, 26(2):214–226, June 2007.
- [8] Zahra Toony, Denis Laurendeau, and Christian Gagné. Pgp2x: Principal geometric primitives parameters extraction. In *Proc. of the 10th International Conference on Computer Graphics Theory and Applications (GRAPP)*, 2015.